Intercombination and forbidden transition rates in C- and N-like ions (O^{2+}, F^{3+}, and S^{9+}) measured at a heavy-ion storage ring

E. Träbert,[1,*] A. G. Calamai,[2] J. D. Gillaspy,[3] G. Gwinner,[4] X. Tordoir,[5] and A. Wolf[4]

[1]*Experimentalphysik III, Ruhr-Universität Bochum, D-44780 Bochum, Germany*
[2]*Department of Physics, Saint Joseph's University, Philadelphia, Pennsylvania 19131*
[3]*National Institute of Standards and Technology, Gaithersburg, Maryland 20899*
[4]*Max-Planck-Institut für Kernphysik, D-69117 Heidelberg, Germany*
[5]*Physique Nucléaire Expérimentale, Université de Liège, B-4000 Liège, Belgium*

Rates of an intercombination transition and several electric-dipole forbidden transitions between the levels of the ground complex in C-like ions of O and F and in N-like ions of S have been measured optically at a heavy-ion storage ring. The lifetime results, 1.250(13) ms for the $2s2p^3$ $^5S_2^o$ level in O^{2+}, 530(25) and 304(5) ms for the $2s^2$ $2p^2$ ^1S_o level in O^{2+} and F^{3+}, respectively, and 5.20(15) and 2.10(6) ms for the $2s^22p^3$ $^2P_{1/2,3/2}^o$ levels of S^{9+}, agree with only some of the theoretical predictions, while they have a lower estimated uncertainty than all of them.

PACS number(s): 32.70.Cs, 39.90.+d, 31.50.+w

I. INTRODUCTION

''Forbidden'' lines, that is, spectral lines from transitions that are forbidden by the electric-dipole (E1) transition selection rules, are of great interest since Edlén [1] identified the famous coronal lines in the visible spectrum of the solar corona with precisely this transition type. For plasma physics, the same physical background opened an observational window into hot plasmas that was to become important several decades later, with the advent of fusion plasma experiments [2]. The energies of many levels in the ground configurations of few-electron ions of elements up to the iron group have also been systematized by Edlén [3–5], so that the wavelengths of magnetic dipole (M1) and electric quadrupole (E2) transitions are well known even for those ions that are not directly observed in solar or terrestrial plasmas.

Regarding the rates of such forbidden transitions, their calculation for a long time was considered easy and reliable, whereas experiment, at least for light ions, seemed unable to deliver precise data. In the nonrelativistic, single-configuration limit, the transition rate is easily calculated from angular coupling factors (Racah algebra) and the transition energy [6]. However, most real atomic systems need a multiconfiguration description, and then the calculations can become very complex [7–10]. As mixings in complex configurations are important and very sensitive to level energies, it has become customary to adjust the calculated term values to the experimental ones within the calculations before determining transition probabilities.

The simplest ions that feature the most prominent M1/E2 lines are the B- and F-like ions with only a single forbidden transition between the two fine-structure levels of the ground configuration. Lifetime measurements on such ions have

been done employing various light sources, including our own work at a heavy-ion storage ring [11,12]. In contrast, five levels exist (Fig. 1) in each of the ground configurations of C-like ions ($2s^22p^2$ $^3P_{0,1,2}$, $^1D_2$, and $^1S_0$) and N-like ions ($2s^22p^3$ $^4S_{3/2}^o$, $^2P_{1/2,3/2}^o$, and $^2D_{3/2,5/2}^o$).

M1 and E2 transitions can occur as contributions to a joint decay channel (see, for example, the aforementioned study on B- and F-like ions [12]), or as separate decay branches with branching ratios that vary markedly with the nuclear charge (as is the case in the examples covered in this study). It is therefore valuable to study similar transitions in several ions of an isoelectronic sequence, as we do with O^{2+} and F^{3+}. However, the strong dependence of the transition wave-
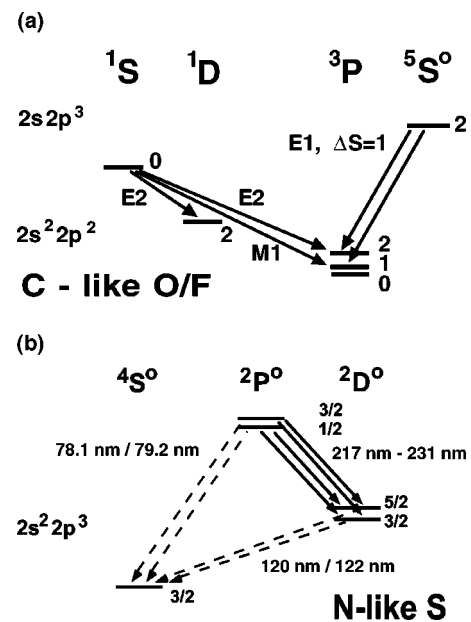

FIG. 1. Simplified level schemes of the atomic systems studied here. (a) C-like ions (O^{2+}, F^{3+}), (b) N-like ions (S^{9+}). Full arrows denote transitions observed here, dashed arrows denote competing decays not directly observed; (b) also shows transition wavelengths.

*Corresponding author. Present address: IPNE, Université de Liège, Sart Tilman B-15, B-4000 Liège, Belgium. Email address: elmar@mbox.pne.ulg.ac.be

lengths and rates on the nuclear charge restricts experimental access for each experimental apparatus with a given set of detectors and filters. In the present study we can observe the decay of the $^1S_0$ level in C-like O^{2+} at both the 436.3 nm line (transition to the $^1D_2$ level) and the 232.1 nm line (transition to the $^3P_1$ level), as well as the corresponding lines for C-like F^{3+} at 353.3 and 187.6 nm. (As our measurements do not involve precise spectroscopy, all of these quoted wavelength values are approximate and for identification only; precise level and wavelength data are available from solar observations and data systematizations and can be found in the NIST atomic structure database.) The $^1S_0$ levels in O^{2+} and F^{3+} are predicted to have lifetimes of ≈ 500 and ≈ 300 ms, respectively. Some of the calculations exceed this range by a factor of 2 to 2.5. The $^1D_2$ level lifetime has been studied in a more highly charged ion, Si^{8+} [13], and the $^1S_0$ level lifetime in a companion study on the O-like ion F^+ [14]. For N-like ions, the decays of the $2s^22p^3\ ^2P^o_{1/2,3/2}$ levels to $^2D^o_{3/2,5/2}$ were accessible by our equipment in S^{9+}, at wavelengths 216 to 226 nm. There are six calculations [10,15–19] that predict lifetimes of ≈ 5 and ≈ 2 ms, respectively. Although our apparatus cannot spectrally resolve the UV-decay branches of the two levels, it is expected that both of the lifetimes can be extracted from a joint decay curve of high statistical reliability.

For C-like O^{2+}, the spin-changing (intercombination) E1 decay of the $2s2p^3\ ^5S^o_2$ level at 166 nm has also been observed. This level, with its lifetime in the 1–2-ms range, was studied earlier by Johnson *et al.* using a radio-frequency (RF) ion trap [20]. This ion has been extensively discussed in the context of solar spectroscopy [21], and the decays of this particular level have been proposed as tools for the interpretation of various astrophysical objects like gaseous nebulae, symbiotic stars, and quasistellar objects, complementing the information to be obtained from forbidden transitions within the ground configuration [22].

II. EXPERIMENT

Our experiment employed a heavy-ion storage ring (TSR at the Max Planck Institute for Nuclear Physics, at Heidelberg, Germany) using the procedures described previously [11–14,23–25]. All ion beams of oxygen, fluorine, and sulphur were produced as negative ions from a sputter-type ion source, accelerated in the first half of a tandem accelerator, stripped to the desired charge state in a gas stripper, and accelerated further to final energies of 6.13 MeV for O^{2+}, 11.61 MeV for F^{3+}, and 20 MeV for S^{9+}, respectively. The sulphur ion beam was stripped to its final charge state in a foil stripper after the accelerator. In all cases, only a selected charge-state ion beam was transported to the storage ring, injected (using multiturn injection so as to increase the number of ions stored), and left coasting for 200 ms to 3 s, depending on the atomic lifetime sought. Then the beam was dumped and the procedure repeated. The stored ion currents reached up to about 100 μA for O^{2+}, 150 μA for F^{3+}, and 80 μA for S^{9+}.

A few-percent fraction of the ion beam was expected to be in excited levels; the fraction originates from the stripping and excitation processes taking place inside (O^{2+}, F^{3+}) or after the injector (S^{9+}), respectively. The ion beam travels about 100 m from the injector to the ion storage ring, which at these ion energies takes 5 to 10 μs, which is about twice the revolution time (6.7 μs for O^{2+}, 5 μs for F^{3+}, 2.2 μs for S^{9+}) of the ions in the storage ring (circumference 55 m). Injection extends over ≈ 0.3 ms with effective stacking of ions being possible over ≈ 30 turns [26]; the pulsed magnetic field used to inflect the ions settles down at ≈ 0.8 ms after the start of the injection. After the end of the settling time the ions are stored on stable orbits.

The storage time constants (limited by collisional losses) depend on the background gas pressure (here a few times 10^{-11} mbar); they were about 13 s for O^{2+}, 23 s for F^{3+}, and 10 s for S^{9+}, as measured by various techniques [11,13,24] (with an accuracy of about 10%). The ion-beam lifetime is important as a systematic correction of the apparent optical decay data. For the $^2P^o$ level decay times in S^{9+}, as well as for the $^5S^o_2$ level decay time in O^{2+}, which are both of the order of a few milliseconds, this correction amounts to about 10^{-4} and thus is practically negligible. For the $^1S_0$ level decay times in O^{2+} and F^{3+}, which are in the few-hundred-ms range, the finite lifetime of the stored ion beam implies a systematic shift at the few-percent level. The full injection and settling time (0.8 ms) is faster than the shortest of the expected radiative lifetimes of present interest, but very long compared to practically all cascade transitions. Higher-lying levels, to which ions can be excited in the stripper, mostly have lifetimes that are much shorter than the travel time to the storage ring; hence their population will have decayed to the ground configuration (of which we observe fine-structure levels) before observation begins. We did not find signs of slow or fast cascades in our data. However, in the case of S^{9+}, we noticed a small additional decay component in the stored ion signal from the beam profile monitor (BPM) that had about 6 % of the total beam amplitude and lasted for about 2 ms after injection. This possibly reflects either a different settling-down behavior of a beam of highly charged ions, or a different initial response of the BPM under such conditions. In any case, it calls for caution in the data evaluation (see discussion below).

We used optical observation in a side-on geometry, through a sapphire window positioned at a distance of 5 cm from the average ion trajectory. In order to boost the signal rate, a light collection system was employed [23]. This simple trough-shaped reflector (made up of an elliptical cross section, with the cylinder axis oriented along the beam trajectory) enhances light collection by about a factor of 2. The light was detected by photomultiplier tubes with 25-mm diameter windows and inherent dark rates of 1 cps (solar-blind type EMR 541 Q for UV light) and about 50 cps (bialkali-metal type EMR 541 N for visible and near-UV light), respectively. Interference filters were used with the EMR 541 N phototube; a filter centered at 436 nm had a peak transmittance of 50%, whereas another filter at 350 nm transmitted only 22%. As some visible stray light (from vacuum gauges and light leaks elsewhere in the ring) was present, it was necessary to employ these filters with the bialkali-metal

TABLE I. Transitions studied and photomultipliers (PM) and filters used. ''vis'' and ''uv'' indicate the two photomultipliers that are sensitive to visible and ultraviolet light, respectively.

	Transition		Wavelength	PM	Filter
Upper level		Lower level	λ (nm)		λ (nm)
O^{2+}					
$2s^2 2p^2\ {}^1S_0$	$\rightarrow$	$2s^2 2p^2\ {}^1D_2$	436.5	vis	436
$2s^2 2p^2\ {}^1S_0$	$\rightarrow$	$2s^2 2p^2\ {}^3P_1$	232.2	uv	
O^{2+}					
$2s 2p^3\ {}^5S_2^o$	$\rightarrow$	$2s^2 2p^2\ {}^3P_{1,2}$	166.1/166.6	uv	a
F^{3+}					
$2s^2 2p^2\ {}^1S_0$	$\rightarrow$	$2s^2 2p^2\ {}^1D_2$	353.3	vis	350
$2s^2 2p^2\ {}^1S_0$	$\rightarrow$	$2s^2 2p^2\ {}^3P_1$	187.6	uv	a
S^{9+}					
$2s^2 2p^3\ {}^2P_{1/2}^o$	$\rightarrow$	$2s^2 2p^3\ {}^2D_{3/2}^o$	226.1	uv	
$2s^2 2p^3\ {}^2P_{3/2}^o$	$\rightarrow$	$2s^2 2p^3\ {}^2D_{3/2}^o$	222.8	uv	
	$\rightarrow$	$2s^2 2p^3\ {}^2D_{5/2}^o$	217.4	uv	

[a]Light path evacuated.

photomultiplier tube in order to reduce the background signal. The solar-blind EMR 541 Q phototube, in contrast, has an upper wavelength sensitivity limit near 270 nm; the lower wavelength cutoff was 150 nm, as given by the sapphire window material of the storage ring vessel (when the light path between the window and the photomultiplier was evacuated). Filters for some of the wavelengths of interest in the UV range were available, but not used, as no stray light in this wavelength region was noted. However, it was ascertained with both spectral lines of interest that have wavelengths below 200 nm that air in the light path effectively blocked the light of interest (establishing also the detector dark rate under storage ring conditions), and that only under the proper vacuum did the photomultiplier detect the desired radiation. Table I summarizes the photomultiplier and filter combinations used on the various transitions.

Each detection cycle was started about 1 ms before injection, and events were sorted into 1000 bins of 0.05-ms width each for the measurement of short lifetimes, and into 300 to 480 bins of 5-ms width each for the long ones. After the experiences from earlier accelerator runs in which many data sets were collected over a few hours each, and the stability and reproducibility confirmed, the present data were taken in a few extended runs (though intermediate accumulated data storage took place every minute). For example, the single decay curve data set on the $O^{2+}\ {}^5S_2^o$ level (Fig. 2) represents 8 h of recording time, and the data in Fig. 3 required 16 h of data accumulation. For O^{2+} and F^{3+}, the accumulated signal reached up to more than 10^5 counts above background.

S^{9+} features a number of forbidden transitions in the ground complex, two of which fall into our present detection range. The decays of the $^2P_{1/2,3/2}^o$ levels to the ground level $^4S_{3/2}^o$ lie in the extreme-ultraviolet (EUV) range and are not presently accessible to us, but the decays to the $^2D_{3/2,5/2}^o$
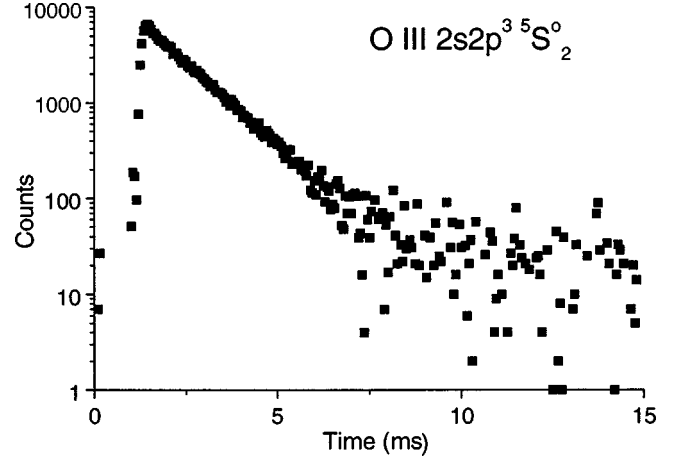

FIG. 2. Photon signal (logarithmic scale) obtained with O^{2+} ions of 6.13 MeV and a solar blind phototube. The data are dominated by the decay of the $2s 2p^3\ {}^5S_2^o$ level. The displayed data represent 300 (out of 1000) data channels of a 8-h run that collected data for about 8 s per channel. A background of 1000 counts per channel [composed of dark rate, spectral contamination (see text) and temporary electronic noise] has been subtracted for the display. Ion injection begins about 1 ms after data taking.

levels at 217, 223, and 226 nm are. The lines are not spectrally resolved, nor are the upper levels very different in lifetime. However, the predicted lifetimes are in the optimum working range of the storage ring technique, and the accumulated signal yielded good statistical reliability. More than 10^6 counts above background were gathered within 30 h of data accumulation.

III. DATA EVALUATION AND RESULTS

The data sets [for samples, see Figs. 2, 3, 4, and 5(a)] were collected and evaluated individually. Nonlinear least-squares fits of one, two, or three exponential components (plus a constant background) were tried by using different algorithms on the full data sets, and also on various subsets: these included truncation of the background tail, which yielded no observable differences, and sequential truncation of up to 10 early data channels (0.5 and 50 ms, respectively) after the curve maximum. Truncating the very first few channels removes data channels that might be affected by the injection process and the subsequent stabilization of the coasting ion beam in the storage ring. When the evaluation was restricted to data recorded later than 0.2 ms after the end of the injection, the lifetime results for the low charge-state ions (as a function of starting channel) varied only within the statistical uncertainty of the individual data set. This time interval is comparable to that found in earlier heavy-ion storage ring work [23,11].

A somewhat more complicated situation is encountered for the $^2P_{1/2,3/2}^o$ levels in S^{9+}. First, the decays of the two levels with lifetimes of 2 and 5 ms, respectively, cannot be spectrally separated, yielding a two-component decay curve [see Fig. 5(a)]. Second, for the S^{9+} beam a slight nonexponential decrease of the ion-beam current was observed during the first about 5 ms of storage [see Fig. 5(b)]. Some of the
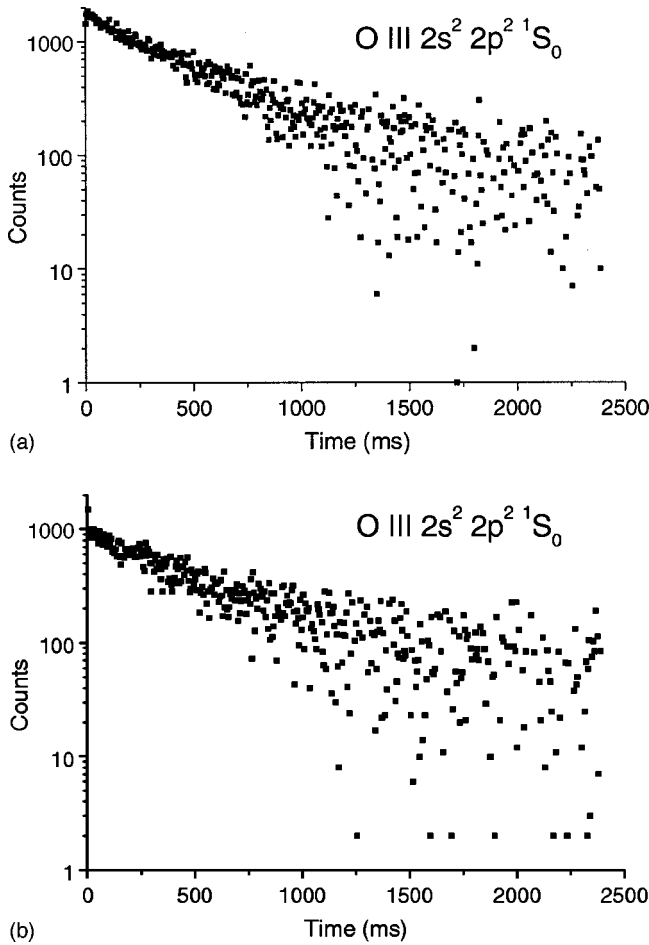
(a)

(b)

FIG. 3. Photon signal (logarithmic scale) obtained with O^{2+} ions of 6.13 MeV. (a) E2 transition $2s^2 2p^2$ $^1D_2 - ^1S_0$, observation through a filter for 436-nm light, observation time 120 s per channel; (b) M1 232-nm decay branch to the $2s^2 2p^2$ $^3P_1$ level, observation without filter for an accumulated time of 80 s per channel. A background of 8450 (a) or 6420 counts (b) per channel has been subtracted from the data. The decay curve of Fig. 2 corresponds to part of the very first channel (at $t=0$, not displayed) of data set (b).

FIG. 4. Photon signal (logarithmic scale) obtained with F^{3+} ions of 11.61 MeV. (a) E2 transition $2s^2 2p^2$ $^1D_2 - ^1S_0$ at 353 nm, observation for about 108 s per channel, with filter; (b) M1/E2 transition to the $2s^2 2p^2$ $^3P_{1,2}$ levels, at 187.6 nm, observation for about 32 s per channel, without a filter. The 300 data channels are 5 ms wide. A background of 1380 counts per channel has been subtracted from curve (a), 75 counts from curve (b).

data runs can better be fitted by taking into account a third decay component (with a decay time of about 0.35 ms) describing the fast loss of a fraction of the freshly stored ion beam. This leads to relatively large errors of $\approx 3\%$ for both level lifetimes. For all other decay curve data of the present study, a single exponential component (plus a constant background) yielded the best fit.

This statement includes the case of O^{2+}, in which the filterless observation of the intercombination decay (at 166 nm, with the light path evacuated) did not preclude some signal of the 232-nm line from entering the data set. However, the evaluation range of the fast signal (Fig. 2) is only about 1/30 of a single lifetime of the blending line (Fig. 3), and thus practically indistinguishable from a constant background. On the other hand, observing the decay of the long-lived level, the blend with the decay of the short-lived level would affect only the very first data channel, which is discarded anyway because of the injection process. However, the admission of ambient air into the light path effectively
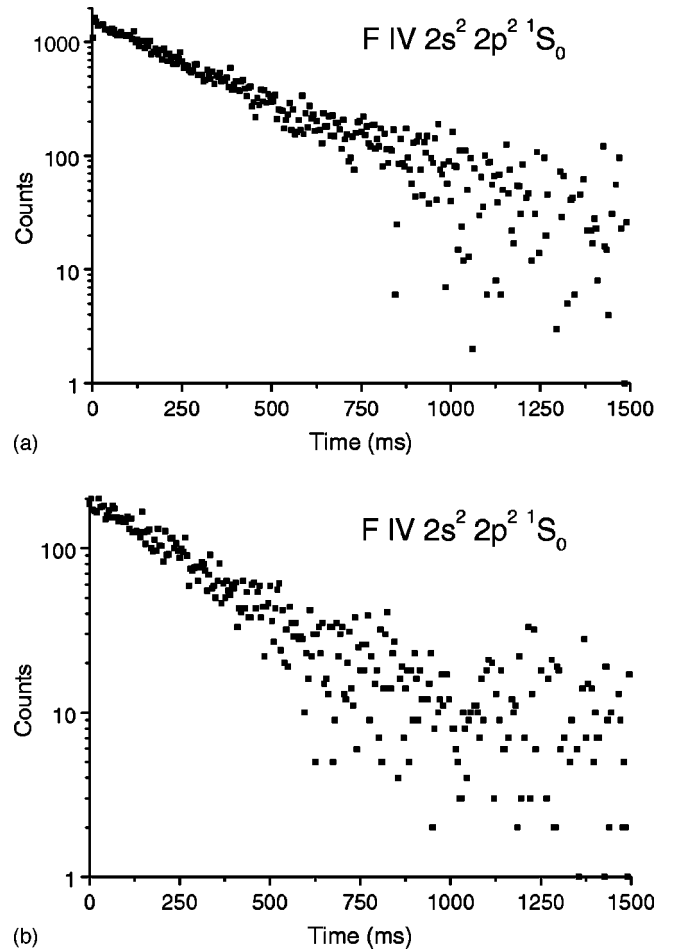
blocked this possible 166-nm contamination straightaway.

Of the S^{9+} $^2P^o_{1/2,3/2}$ levels, the $J=3/2$ level has the shorter lifetime and thus the higher transition probability. Assuming statistical level populations proportional to $g=2J+1$, the expected decay amplitudes (initial intensities of the decay components), would be about 4:1 in favor of the 2-ms lifetime component. However, the actual branching fraction of the (observed) UV branch is somewhat higher for the 5-ms component ($J=1/2$ level) than for the other [19]. This interplay is, indeed, reflected in the relative amplitudes of the fit components, as well as in the final lifetime errors (see below).

To obtain the radiative lifetimes in the rest frame of the ions, a correction for relativistic time dilation ($\gamma = 1.000\,41$ for 6.13 MeV $^{16}O^{2+}$, $1.000\,66$ for 11.61 MeV $^{19}F^{3+}$, and $1.000\,67$ for 20 MeV $^{32}S^{9+}$, respectively) was applied, but made little difference at the present level of precision.

In the cases where we have several independent decay curves, we derive the final results for the radiative decay rates as the weighted means of the individual results. After
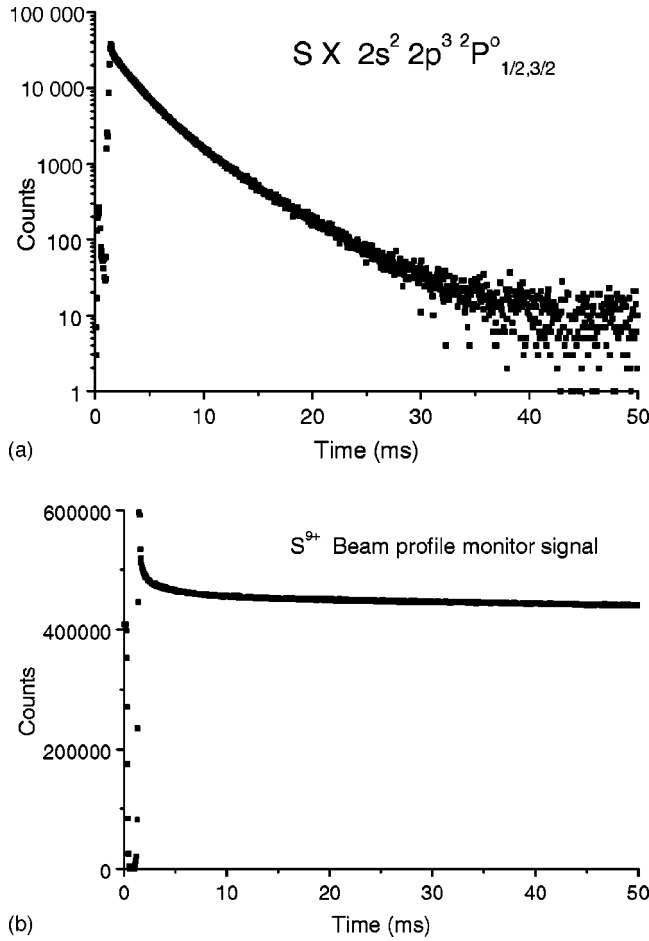
(a)

(b)

FIG. 5. (a) Photon signal (logarithmic scale) obtained with S^{9+} ions of 20 MeV. The signal stems from the spectrally unresolved decays $2s^2 2p^3$ $^2D^o_{3/2,5/2} - ^2P^o_{1/2,3/2}$ at 217, 226, and 223 nm, respectively. The data shown represent the sum of all data and thus a collection time of about 25 s per channel. A background of 35 counts has been subtracted. The two-component character (plus an initial fast component of a 0.2-ms lifetime) of the decay curve is evident. (b) Beam profile monitor signal. Within the first 2 ms of the displayed data, the end of the preceding cycle, ion dumping, fresh filling with initial losses, and settling of the injected ion beam to stable conditions are recognizable, both here and in the corresponding photon signal (a).

correcting the observed photon signal decay rates for the ion-beam loss rates, the results for the total decay rates are converted to the atomic level lifetimes given in Tables II, III, and IV: (530 ± 25) ms for the $2s^2 2p^2$ $^1S_0$ level of O^{2+} and (304 ± 5) ms for the same level in F^{3+}, (1.25 ± 0.013) ms for the $2s 2p^3$ $^5S_2^o$ level in O^{2+}, and (2.10 ± 0.06) and (5.20 ± 0.15) ms for the $2s^2 2p^3$ $^2P^o$ $J = 3/2$ and $J = 1/2$ levels in S^{9+}, respectively. Our final (1σ) errors are dominated by the statistical uncertainties. The uncertainties due to the storage time correction, to the reproducibility of the lifetime data with fits to truncated data sets, and to the background contribution are all much smaller than these stated errors.

The observed spectral lines make up the full fine-structure interval of several eV. This is many orders of magnitude larger than any possible Zeeman shifts of the levels in the

TABLE II. Mean lives τ of the $2s^2 2p^2$ $^1S_0$ level in C-like ions of O and F.

Ion	τ (ms)	Ref.
O^{2+}		
Theory		
	546	[28,29]
	527	[32]
	1333	[27]
	517	[33]
	1269	[15]
	546	[34]
	546	[7]
	392	[30] Table XII/XIV
	519	[30] Table X
	559 ± 56	[35]
Experiment		
	(530 ± 25)	This work
F^{3+}		
Theory		
	312	[28]
	608	[15]
	310	[7]
	299	[30] Table XII/XIV
	312 ± 31	[35]
Experiment		
	(304 ± 5)	This work

magnetic fields of the ion-beam guidance system. Therefore any notable effect on the measured atomic lifetimes, by the Zeeman mixing of the levels of interest (with a level of infinite lifetime, the ground level) can be safely excluded.

IV. DISCUSSION AND OUTLOOK

For the M1/E2 transitions presented here, our measurements are the only ones so far, and comparison therefore is possible only with theory (Tables II and III). For the two C-like ions, most of the theoretical data cluster in a range near 500 ms (O^{2+}) and 300 ms (F^{3+}), respectively, which is confirmed by experiment. However, the experiment is much more precise than the scatter range of the calculations. Most of the calculations of transition probabilities for M1/E2 transitions that were investigated here carried no error estimate at all. The early calculation by Cheng, Kim, and Desclaux [15] is off by a factor of 2, as is the calculation by Bhatia, Doschek, and Feldman [27]. In contrast, the even older calculations by Garstang [28,29] differ from the experimental finding by less than 10%. It is interesting to note that several of the theoretical results have been obtained from the same codes, like SUPERSTRUCTURE or CIV3, but with very different results. We also note that the paper by Vilkas *et al.* [30] has two sets of data (from differently tailored calculations for some elements) that do not agree with each other.

TABLE III. Mean lives τ of the $2s^2 2p^3\ ^2P^o$ levels in the N-like ion S^{9+}.

	Level	τ (ms)	Ref.
	$^2P^o_{1/2}$		
Theory			
		4.84	[15]
		5.12	[16]
		5.06	[10]
		5.30	[17]
		5.10	[18]
		5.28	[19]
Experiment			
		(5.20±0.15)	This work
	$^2P^o_{3/2}$		
Theory			
		2.00	[15]
		2.11	[16]
		2.11	[10]
		2.18	[17]
		2.13	[18]
		2.16	[19]
Experiment			
		(2.10±0.06)	This work

Our experimental data for O^{2+} corroborate the semiempirically adjusted data in their Table X rather than the combination of their purely theoretically derived Tables XII and XIV. It appears fortuitous that both our data and the calculations are more accurate in the case of F^{3+} than in the case of O^{2+}.

For our measurement on N-like sulphur, the data analysis

TABLE IV. Mean life τ of the $2s2p^3\ ^5S^o_2$ level in the C-like ion O^{2+}.

	τ (ms)	Ref.
Theory		
	1.85	[15]
	0.98	[15] after wavelength correction
	1.75	[27,36]
	0.67	[31]
	1.43	[7]
	1.36	[22]
	1.67	[21]
	1.72	[37]
	1.21±0.06	[38]
	1.22	[39]
Experiment		
	(1.22±0.08) (2σ)	[20]
	(1.250±0.013) (1σ)	This work

is hampered by the complication of two spectrally unresolved decays contributing to a joint decay curve, with decay constants that are not very different from each other. Only thanks to the good statistical quality of the data (signal-to-noise ratio as well as high accumulated signal) does the combined fit yield rather precise lifetime results for both levels. The convergence of many calculations, even with only a few configurations, is much faster with highly charged ions than with almost neutral ones. Consequently, the relatively simple multiconfiguration Dirac-Fock (MCDF) calculations by Cheng *et al.* [15] feature results that are not so different from the newer ones that employed a high number of configurations in large-scale calculations. Our measurement now shows that all these calculations are rather accurate.

Besides the $2s^2 2p^3\ ^2P^o_{1/2,3/2}$ levels studied here, there are two more excited levels, $^2D^o_{3/2}$ and $^2D^o_{5/2}$, in the ground configuration of S^{9+}. The $^2D^o_{3/2}$ level has a predicted lifetime near 70 ms, which is in easy reach of the storage ring technique, while the $^2D^o_{5/2}$ level has a predicted lifetime between 2 and 3 s, pushing the performance envelope of the technique. However, both levels feature decays only in the vacuum ultraviolet, at wavelengths of about 120 nm. This is shorter than the cutoff wavelength of the presently employed sapphire windows in the storage ring vessel. A new detection system inside the vacuum vessel could give access to these transitions.

The data on the intercombination decay of the $2s2p^3\ ^5S^o_2$ level in O^{2+} corroborate the earlier data by Johnson *et al.* [20] that were obtained with an RF ion trap. However, the new data are more precise by a factor of 3. The results compare fairly well with some of the many theoretical predictions (Table IV). Among the theoretical predictions, the 20-year-old multiconfiguration Dirac-Fock calculations by Cheng, Kim, and Desclaux [15] show considerable deviations from both more recent calculations and from our experimental results on O^{2+} and F^{3+}, that is, for ions that are close to the neutral end of the iso-electronic sequence. These researchers were opening up the field of MCDF calculations at the time, and while their early results were very useful for surveys and a first orientation, their calculations obviously are at their limit of applicability with low-charge ions. For the $2s2p^3\ ^5S^o_2$ level in O^{2+} these old calculations have the additional problem of probably using too few configurations to deal adequately with excited levels, among which the level under present investigation is meanwhile known to cause particular computational problems. As an indicator of reliability we take the calculated transition wavelength that is off from the experimentally known value by about 20%. Correcting the prediction for the transition rate by the dependence on the third power of the transition energy changes the lifetime predictions from 1.85 to 0.98 s. Almost all other predictions—and the experimental results—lie inside this interval.

The same problem of an insufficient number of configurations included in the computation may be suspected to cause the discrepancy for the results presented by Cowan, Hobbs, and York [31]. Cowan's suite of Hartree-Fock programs has meanwhile been used by many people and often

gives very useful results. However, our various heavy-ion storage ring lifetime data on intercombination decays [23,11,24,25] indicate that many results in this particular early survey paper for the astrophysical community are off by factors of 2 to 3 from the bulk of other calculations and from experiment. In contrast, Garstang's older calculations [28,29] come close to our experimental findings. None of the old calculations, however, included systematic tests of convergence or were quoted with meaningful error estimates.

The scatter of theoretical predictions filling the aforementioned interval illustrates the problems this quintet level poses for theorists. However, more than a decade after the RF ion trap measurements by Johnson *et al.* [20], there are two calculations [38,39] that agree with experiment very well. We note that these calculated results are slightly shorter than our experimental lifetime value. Just the same was found in our preceding study on the same level in N^+; since then, some new calculations [40] have moved theory closer to our experimental finding [24].

Reviewing the optical lifetime measurements that have been done at the TSR heavy-ion storage ring so far, there are now precise intercombination transition data on B^+ and C^{2+} (Be-like ions) [23,11], C^+ and N^{2+} (B-like) [25], N^+ [24] and, from this work, O^{2+} (C-like), as well as Al^+ (Mg-like) [11], mostly with a precision better than 1%. Moreover, lifetime data with a precision in the few-percent range have been obtained on forbidden decays in B-like ions (Ti^{17+} [12]), C-like ions (O^{2+}, F^{3+} (this work), Si^{8+} [13]), N-like ions [S^{9+} (this work)], O-like ions (F^+ [14], Si^{6+} [13]), and F-like ions (Sc^{12+} [11], Ti^{13+} [12]). The storage ring data regularly exceed the precision of published calculations and thus provide an incentive for renewed theoretical studies, particularly now that benchmark data have become available in previously unexplored regions.

[1] B. Edlén, Z. Astrophys. **22**, 30 (1942).

[2] B. Edlén, Phys. Scr., T **8**, 5 (1984).

[3] B. Edlén, Phys. Scr. **22**, 593 (1981).

[4] B. Edlén, Phys. Scr. **26**, 71 (1982).

[5] B. Edlén, Phys. Scr. **30**, 135 (1984).

[6] L. J. Curtis, Phys. Scr., T **8**, 77 (1984).

[7] C. Froese Fischer and H. P. Saha, Phys. Scr. **32**, 181 (1985).

[8] K. L. Baluja, J. Phys. B **18**, L413 (1985).

[9] K. L. Baluja and C. J. Zeippen, J. Phys. B **21**, 1455 (1988).

[10] C. J. Zeippen, Mon. Not. R. Astron. Soc. **198**, 111 (1982).

[11] E. Träbert, A. Wolf, J. Linkemann, and X. Tordoir, J. Phys. B **32**, 537 (1999).

[12] E. Träbert, G. Gwinner, X. Tordoir, A. Wolf, and A. G. Calamai, Phys. Lett. A **264**, 311 (1999).

[13] E. Träbert, A. Wolf, E. H. Pinnington, J. Linkemann, E. J. Knystautas, A. Curtis, N. Bhattacharya, and H. G. Berry, Can. J. Phys. **76**, 899 (1998).

[14] A. G. Calamai, G. Gwinner, X. Tordoir, E. Träbert, and A. Wolf, Phys. Rev. A **61**, 062508 (2000).

[15] K.-T. Cheng, Y.-K. Kim, and J. P. Desclaux, At. Data Nucl. Data Tables **24**, 111 (1979).

[16] M. Eidelsberg, F. Crifo-Magnant, and C. J. Zeippen, Astron. Astrophys., Suppl. Ser. **43**, 455 (1981).

[17] M. Godefroid and C. Froese Fischer, J. Phys. B **17**, 681 (1984).

[18] S. R. Becker, K. Butler, and C. J. Zeippen, Astron. Astrophys. **21**, 375 (1989).

[19] G. Merkelis, I. Martinson, R. Kisielius, and M. J. Vilkas, Phys. Scr. **59**, 122 (1999).

[20] B. C. Johnson, P. L. Smith, and R. D. Knight, Astrophys. J. **281**, 477 (1984).

[21] S. O. Kastner, W. E. Behring, and A. K. Bhatia, Astrophys. J., Suppl. Ser. **53**, 129 (1983).

[22] H. Nussbaumer and P. J. Storey, Astron. Astrophys. **99**, 177 (1981).

[23] J. Doerfert, E. Träbert, A. Wolf, D. Schwalm, and O. Uwira, Phys. Rev. Lett. **78**, 4355 (1997).

[24] E. Träbert, A. Wolf, E. H. Pinnington, J. Linkemann, E. J. Knystautas, A. Curtis, N. Bhattacharya, and H. G. Berry, Phys. Rev. A **58**, 4449 (1998).

[25] E. Träbert, G. Gwinner, E. J. Knystautas, X. Tordoir, and A. Wolf, J. Phys. B **32**, L491 (1999).

[26] G. Bisoffi *et al.*, Nucl. Instrum. Methods Phys. Res. A **287**, 320 (1990).

[27] A. K. Bhatia, G. A. Doschek, and U. Feldman, Astron. Astrophys. **76**, 359 (1979).

[28] R. H. Garstang, Mon. Not. R. Astron. Soc. **111**, 115 (1951).

[29] R. H. Garstang, in *Planetary Nebulae*, edited by D. E. Osterbrock and C. R. O'Dell, International Astronomical Union Symposium No. 34 (Reidel, Dordrecht, 1968), p. 143.

[30] M. J. Vilkas, I. Martinson, G. Merkelis, G. Gaigalas, and R. Kisielius, Phys. Scr. **54**, 281 (1996).

[31] R. D. Cowan, L. M. Hobbs, and D. G. York, Astrophys. J. **257**, 373 (1982).

[32] H. Nussbaumer, Astrophys. J. **166**, 411 (1971).

[33] H. Nussbaumer and C. Rusca, Astron. Astrophys. **72**, 129 (1979).

[34] K. L. Baluja and J. G. Doyle, J. Phys. B **14**, L11 (1981).

[35] M. E. Galavís, C. Mendoza, and C. J. Zeippen, Astron. Astrophys., Suppl. Ser. **123**, 159 (1997).

[36] A. K. Bhatia and S. O. Kastner, At. Data Nucl. Data Tables **54**, 133 (1993).

[37] K. M. Aggarwal, A. Hibbert, and F. P. Keenan, Astrophys. J., Suppl. Ser. **108**, 393 (1997).

[38] J. Fleming and T. Brage, J. Phys. B **30**, 1385 (1997).

[39] C. Mendoza, C. J. Zeippen, and P. J. Storey, Astron. Astrophys., Suppl. Ser. **135**, 159 (1999).

[40] C. Froese Fischer, Phys. Scr., T **83**, 49 (1999).